Springer

Journal of
Mechanical
Science and
Technology

Journal of Mechanical Science and Technology 22 (2008) 991~998

www.springerlink.com/content/1738-494x

Multi-dimensional modeling of CO poisoning effects on proton exchange membrane fuel cells (PEMFCs)

Hyunchul Ju[1], Kwan-Soo Lee[2] and Sukkee Um[2,*]

[1]*Department of Mechanical Engineering Inha University 253 Yonghyun-dong, Nam-Gu, Incheon, 402-751, Korea*
[2]*School of Mechanical Engineering Hanyang University 17 Haengdang-dong, Seongdong-gu, Seoul 133-791, Korea*

(Manuscript Received August 6, 2007; Revised February 11, 2008; Accepted February 11, 2008)

Abstract

Carbon monoxide (CO), which is preferentially absorbed on the platinum catalyst layer of a proton exchange membrane fuel cell (PEMFC), is extremely detrimental to cell performance. Essentially, the carbon monoxide absorption diminishes the cell's performance by blocking and reducing the number of catalyst sites available for the hydrogen oxidation reaction. In order to obtain a full understanding of CO poisoning characteristics and remediate CO-poisoned PEMFCs, a CO poisoning numerical model is developed and incorporated into a fully three-dimensional electrochemical and transport coupled PEMFC model. By performing CFD numerical simulations, this paper clearly demonstrates the CO poisoning mechanisms and characteristics of PEMFCs. The predictive capability for CO poisoning effects enables us to find major contributors to CO tolerance in a PEMFC and thus successfully integrate CO-resistant fuel cell systems.

Keywords: Fuel cell; Carbon monoxide poisoning; Mass transfer; Platinum catalyst; Onboard reforming system

1. Introduction

Increasing awareness regarding environmental issues and depleting energy reserves has prompted research by industry, government, and academia into diverse possibilities for powering tomorrow's vehicles. Several alternatives exist for the next generation of vehicles. Currently, two of the most promising technologies are the hybrid electric vehicle (HEV) and the fuel cell vehicle (FCV). HEVs are already in commercial production, while the FCV is still in the prototype stage. Although FCV technologies show great promise, the FCV still faces many challenges, most notably cost, durability, and on-board hydrogen storage. Regarding the issue of on-board hydrogen storage for FCVs, high pressure hydrogen storage and metal hydrogen storage technologies have been actively researched so far. While both such storage systems seem attractive and promising, several issues associated with a hydrogen distribution infrastructure and on-board H_2 storage safety remain. Therefore, current research embraces the possibility of onboard reforming of hydrocarbon fuels into hydrogen, as an alternative to direct hydrogen storage. When reformate from onboard reforming systems is used for the feed gas, the incoming hydrogen stream is diluted with nitrogen and carbon dioxide, usually containing a small amount of carbon monoxide (CO) as well. The effects of hydrogen dilution and carbon monoxide (CO) poisoning on anode performance, particularly under high fuel utilization conditions, are significant [1-3]. Furthermore, current catalysts of proton exchange membrane fuel cells (PEMFCs) are tolerant to only 10ppm of CO in the feed gas [4]. CO feed gas levels as low as 25 ppm have shown significant reduction in steady state maximum power when compared to pure H_2 gas, using traditional, pure platinum catalyst [1]. Cells using a combination of Pt and Ru have shown CO tolerances of up to 250 ppm, but the

*Corresponding author. Tel.: +82 2 2220 0432 Fax.: +82 2 2220 0432
E-mail address: sukkeeum@hanyang.ac.kr
DOI 10.1007/s12206-008-0207-1

long-term stability of these catalysts is still questionable [5].

Extensive studies have been performed to evaluate the effects of CO poisoning on the PEMFCs. Springer et al. [2] developed a one-dimensional PEMFC model and investigated CO tolerance of the Pt anode catalyst. In this model, four overall reactions were considered for the adsorption and electro-oxidation of CO and H_2; the effect of air bleeding was, however, not included. A sensitivity analysis of several kinetic parameters was also performed as they greatly influence the CO fractional coverage and H_2 electro-oxidation. Zhang et al. [6] investigated the influence of the anode flow rate and cathode oxygen partial pressure on the PEMFC performance in the presence of CO. They showed that a higher anode inlet flow rate leads to higher anode overpotential and hence lower fuel cell performance. On the other hand, they reported that oxygen crossover through the membrane is partly responsible for the removal of CO from the anode catalyst surface. Camara et al. [7] introduced several models of CO poisoning kinetics: the linear-bonded adsorbed CO model, the bridge-bonded adsorbed CO model, and the linear-bonded CHO and COOH derivative model. They concluded that CO oxidation starts mainly at the bridge-bonded sites, and only at high overpotentials do the linearly adsorbed CO start to be oxidized.

Based on these prior studies, the objective of this study was to develop a three-dimensional, electrochemical-transport fully coupled numerical model of PEMFC with the predictive capability of CO poisoning and associated air bleed processes. The computational capability is intended to provide a design tool for optimizing designing and operating conditions of fuel cells running on CO-containing reformate gas and suggesting optimal air bleed strategies with the best compromise between reduced energy efficiency and enhanced cell performance.

2. Model formulation

2.1 Governing equations

Modeling of CO poisoning effect is based on four chemical/electrochemical processes for the anode reactions: hydrogen and CO adsorption onto metal catalyst sites as well as hydrogen and CO electro-oxidation. The detailed CO poisoning mechanisms were successfully implemented in a three-dimensional comprehensive PEMFC model presented in Um et al. [8] and Ju and Wang [9]. The reader is referred to these papers for a detailed explanation of the numerical model. Accordingly, only a brief summary of the model descriptions and assumptions is repeated here. The governing Eqs. of the PEMFC model are listed in Table 1. As a first attempt for numerical analysis of CO poisoning effects, we ignored thermal and transient effects for simplification. Therefore, the energy equation has not been included and the transient term in each conservation equation was also dropped out in the present study. For species transport equations, hydrogen, water vapor, and CO were solved on the anode side, whereas oxygen and water vapor were solved on the cathode side. Nitrogen was considered as an inert gas throughout the entire cell.

For CO poisoning analysis, the anode kinetic Eqs. should be modified. Springer et al. [2] suggested four kinetic steps on the anode:

Table 1. A single-phase PEMFC model: governing equations with source terms identified in various PEMFC components.

	Conservation Equations	Source Terms			
		Flow Channels	Diffusion Layers	Catalyst Layers	Membrane
Mass	$\nabla\cdot(\rho\vec{u})=0$			$\vec{u}=0$	$\vec{u}=0$
Momentum	$\frac{1}{\varepsilon^2}\nabla\cdot(\rho\vec{u}\vec{u})=-\nabla p+\nabla\cdot\tau+S_u$	$S_u=0$	$S_u=-\frac{\mu}{K}\vec{u}$	$S_u=0$	$S_u=0$
Species	$\nabla\cdot(\vec{u}c_k)=\nabla\cdot(D_k^{eff}\nabla c_k)+S_k$	$S_k=0$	$S_k=0$	$S_k=-\nabla\cdot\left(\frac{\xi_k}{F}i_e\right)-\frac{s_k j}{nF}$	
Charge	$\nabla\cdot(\kappa^{eff}\nabla\Phi_e)+\nabla\cdot(\kappa^{eff}\xi\frac{RT}{F}\nabla\ln a)+S_\Phi=0$	$S_\Phi=0$	$S_\Phi=0$	$S_\Phi=j$	$S_\Phi=0$

Electrochemical Reaction: $\sum_k s_k M_k^z = ne^-$ where $M_k \equiv$ chemical formula of species k; $s_k \equiv$ stoichiometry coefficient; $n \equiv$ number of electrons transferred

$$CO + M \underset{b_{fc}(\theta_{CO})k_{fc}}{\overset{k_{fc}}{\rightleftharpoons}} (M\text{-}CO) \quad (1)$$

$$H2 + 2M \underset{b_{fh}k_{fh}(\theta_{CO})k_{fc}}{\overset{k_{fh(\theta CO)}}{\rightleftharpoons}} 2(M\text{-}H) \quad (2)$$

$$(M-H) \xrightarrow{k_{eh}} H^+ + e^- + M \quad (3)$$

$$H_2O + (M-CO) \xrightarrow{k_{ec}} M + CO_2 + 2H^+ + 2e^- \quad (4)$$

Eqs. (1) and (2) represent adsorption of CO and H_2 on the Pt catalyst, respectively, whereas Eqs. (3) and (4) correspond to H_2 and CO electro-oxidation, respectively. As shown in Eqs. (1) through (4), the hydrogen adsorption rate constant, k_{fh}, and the backward/forward CO adsorption ratio, b_{fc}, are functions of the CO site coverage. In other words, the desorption rate for CO and the adsorption rate for H_2 are assumed to be functions of θ_{CO}. Other kinetic parameters have been assumed to be constant in the following calculations. Eqs. (1) through (4) in conjunction with the species balance laws can be used to derive expressions for θ_{CO} and θ_{H2} that represent the fractions of catalyst sites adsorbed by CO and H_2, respectively. Under the steady state, the transient terms of the following species balance Eqs. are equal to zero:

$$\rho\dot{\theta}_{CO} = k_{fc}P_{CO}(1-\theta_{CO}-\theta_{H2}) - b_{fc}k_{fc}\theta_{CO} - k_{ec}\theta_{CO}e^{\frac{\eta_a}{b_c}} = 0 \quad (5)$$

$$\rho\dot{\theta}_{H2} = k_{fh}P_{H2}(1-\theta_{CO}-\theta_{H2})^n - b_{fh}k_{fh}\theta_{H2}^n - k_{eh}\theta_{H2}\left(e^{\frac{\eta_a}{b_h}} - e^{-\frac{\eta_a}{b_h}}\right) = 0 \quad (6)$$

In the above, n denotes the order of H_2 adsorption step. In the current work, first order H_2 adsorption was considered, i.e., n=1. Using Eqs. (5) and (6), the fractions of catalyst sites adsorbed by CO and H_2 can be solved to result in:

$$\theta_{H2} = (a_2+a_3)/\left[\frac{(a_1+a_2+a_3)}{b_1}\cdot(b_1+b_2+b_3) - a_1\right] \quad (7)$$

$$\theta_{CO} = \frac{a_1\cdot(1-\theta_{H2})}{a_1+a_2+a_3} \quad (8)$$

where coefficients a_1, a_2, a_3, b_1, b_2, and b_3 are defined as follows and all have the units of A/m^2:

$$a_1 = k_{fc}P_{CO} = k_{fc}c_{CO}RT \quad (9)$$

$$a_2 = b_{fc}k_{fc} \quad (10)$$

$$a_3 = k_{ec}\cdot e^{\frac{\eta_a}{b_c}} \quad (11)$$

$$b_1 = k_{fh}P_{H2} = k_{fh}c_{H2}RT \quad (12)$$

$$b_2 = b_{fh}k_{fh} \quad (13)$$

$$b_3 = k_{eh}\left(e^{\frac{\eta_a}{b_h}} - e^{-\frac{\eta_a}{b_h}}\right) \quad (14)$$

In order to account for CO poisoning in the present model, the equation for the volumetric transfer current density generated by hydrogen oxidation is modified to include the fractional coverage of hydrogen on the anode Pt catalyst as a factor; see Eq. (15). Similarly, the electro-kinetic rate equation for CO is given by Eq. (16):

$$j_{H2} = \theta_{H2}\cdot a\cdot k_{eh}\cdot\left(e^{\frac{\eta_a}{b_h}} - e^{-\frac{\eta_a}{b_h}}\right) = \theta_{H2}\cdot a\cdot k_{eh}\cdot\left\{\frac{\alpha_a+\alpha_c}{R\cdot T}\cdot F\cdot\eta_a\right\} \quad (15)$$

$$j_{CO} = \theta_{CO}\cdot a\cdot k_{ec}\cdot e^{\frac{\eta_a}{b_c}} \quad (16)$$

where a is the specific surface area, i.e., the electrochemically active area per unit of the electrode volume. Then, the source terms in various species conservation Eqs. become

$$S_{H2} = -\frac{j_{H2}}{2F} \quad (17)$$

Table 2. Physical parameters used for the analysis of CO poisoning effects.

Parameter	Description	Quantity	Dimension
k_{fc}	Forward CO adsorption rate times 2F	1.0×10^5	A/m^2·atm
b_{fc}	Back-to-forward CO adsorption ratio	4.5×10^{-6}	atm
k_{fh}	Forward H_2 adsorption rate times 2F	1.0×10^6	A/m^2·atm
b_{fh}	Back-to-forward H_2 adsorption ratio	0.5	atm
n	Order of H_2 adsorption step	1	-
k_{ec}	Exchange current density of CO electro-oxidation	2.0×10^{-3}	A/m^2
k_{eh}	Exchange current density of H_2 electro-oxidation	1.0×10^4	A/m^2
a	Specific electro-active area	1.0×10^5	1/m
b_c	Tafel slope for CO electro-oxidation	0.06	V
b_h	Tafel slope for H_2 electro-oxidation	0.06	V

$$S_{CO} = -\frac{j_{CO}}{2F} \tag{18}$$

Finally, the source term in the charge conservation equation for the electrolyte phase potential can be expressed as

$$S_{\Phi} = j_{H2} + j_{CO} \tag{19}$$

2.2 Model parameters

All parameters used in the current work were taken from Springer et al. [2], except that k_{fh} and b_{fc} were assumed to be constant without loss of generality and main physics. Table 2 lists a complete set of the model parameters used in this work.

3. Numerical implementation

3.1 Numerical procedures

For the analysis of CO poisoning effects, both 2-D and 3-D numerical PEMFC codes were developed by using the commercial software, STAR-CD. All calculations were made for a standard single-channel fuel cell (see Ju et al. [10] for its geometry and dimensions) at 80°C. A uniform and orthogonal grid was applied to both 2-D and 3-D computational domains. The numbers shown in Fig. 1 represent the number of elements applied to the 2-D mesh in the direction of x and y. Totally, the 2-D mesh consists of 54×200 elements. For the 3-D mesh, the same number of elements was applied in x-direction. But the number of elements applied in y-direction was halved to reduce the computational time, i.e., from 200 to 100. Fig. 2 displays the grid applied to the 3-D PEMFC geometry along the z direction. A total of 20 elements are used for gas channels, upper current collector, and lower current collector, in the z-direction. Thus, the 3-D mesh is (20×20+34×60)×100.

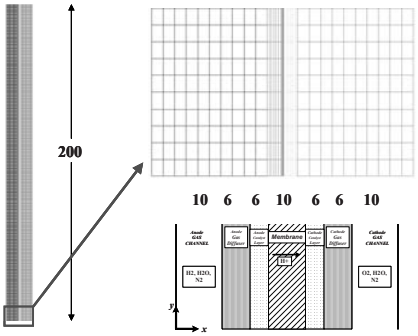

Fig. 1. Schematic diagram and computational mesh for a single channel 2-D PEMFC.

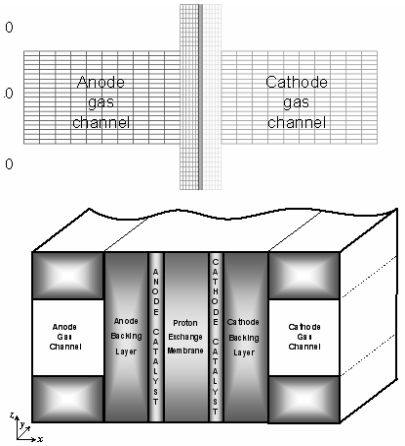

Fig. 2. Schematic diagram and computational mesh for a single channel 3-D PEMFC.

3.2 Numerical behavior in the presence of CO

Generally, the simulation of PEMFCs takes longer under conditions of higher current density or lower cell voltage, because there is higher hydrogen electro-oxidation in the anode and higher water vapor production in the cathode. The numerical simulation of PEMFCs in the presence of CO requires much more computational time. As shown in Table 1, the magnitude of k_{ec}, which is pre-exponential CO electro-oxidation rate, is much smaller than the other kinetic parameters. Physically, this implies that the reaction of CO electro-oxidation, i.e., in Eq. (4), is the slowest one of all anode reactions. As a general rule of thumb, CO and water vapor, which are present in Eq. (4), tend to converge more slowly than other species.

4. Results and discussion

4.1 Main features of CO poisoning

Springer et al. [2] introduced a current density threshold beyond which CO poisoning the Pt catalyst comes into effect. This critical current occurs when the CO coverage reaches a saturation point where its adsorption is balanced only by desorption without resorting to the electro-oxidation. In this limiting case, the CO coverage is maximal and its value can be simply given by

$$\theta_{CO} = 1 - \left(\frac{b_{fc}}{b_{fc} + x_{CO} P_a} \right) \tag{20}$$

as obtained from Eq. (5) by assuming no electro-

oxidation of CO. Under this maximum coverage of CO, there is a minimum current produced by electro-oxidation of H_2 that is sustained by its absorption rate assuming that H_2 desorption is negligible. This current density threshold can thus be derived from Eq. (6) as follows:

$$I_{hl} = k_{fh} x_{H2} P_a \cdot (1-\theta_{CO})^n = k_{fh} x_{H2} P_a \cdot \left(\frac{b_{fc}}{b_{fc} + x_{CO} P_a} \right)^n \quad (21)$$

where n is the order of hydrogen adsorption step. The H_2 coverage, θ_{H2}, has been assumed to be negligibly small in arriving at Eq. (21).

For small current densities, $I<I_{hl}$, the cell voltage-current characteristics are not affected by the poisoned nature of Pt catalyst. This feature is clearly seen in the simulation results to be shown shortly. Only when the cell current density exceeds the threshold value I_{hl} will significant voltage loss and a sharp rise of anode overpotential occur. The high overpotential is used to remove CO from catalyst sites electrochemically. When the cell voltage is further depressed, or equivalently the anode overpotential becomes very large, CO electro-oxidation is greatly accelerated, thereby significantly removing CO from the catalyst sites. Eq. (21) further indicates that the threshold current density is smaller for higher CO concentration. Hence, when the CO concentration in the anode inlet feed increases, the regime of sharp voltage drop begins at lower current densities.

Before discussing CO poisoning simulation results, it should be noted that the kinetic Eqs. are a small fraction of the computer code, but in the presence of CO have a major effect. Springer et al. [11] mentioned the difficulty of measuring the rates of CO electro-oxidation due to the very small magnitude of its value (e.g., k_{ec} = 10nA/cm^2 Pt). Therefore, there may exist a high uncertainty in the value of k_{ec}, while this parameter can significantly influence the magnitude of hydrogen electro-oxidation current obtainable at low voltage. Other parameters such as the forward H_2 adsorption rate, k_{fh}, and the back-to-forward CO adsorption ratio, b_{fc}, are also highly dependent on the fractional coverage of CO, i.e. θ_{CO}. Furthermore, these two parameters directly influence the value of the threshold current density, thus significantly affecting the shape of the polarization curve. Hence, for a CO poisoning simulation, the kinetic parameters used to describe the CO poisoning process should be chosen very carefully and within acceptable ranges recommended in the literature. The basic understanding of the CO poisoning effects is also paramount for matching with experimental data as well as analyzing the detailed simulation results.

Fig. 3 shows the two-dimensional simulation results of the anode overpotential as a function of the current density with various concentrations of CO in the anode feed streams. It is clear that the anode voltage loss is larger with increasing CO con-centration in the hydrogen feed streams. In addition, as discussed earlier, the three distinctive regimes of a CO-poisoned polarization curve are clearly seen in the high CO concentration cases (50ppm CO and 100ppm CO). In the low current density regime (between 0 and 0.4A/cm^2 for 100ppm CO), a relatively small increase in the anode overpotential is observed. As the current density is greater than 0.4A/cm^2 for 100ppm CO and 0.75A/cm^2 for 50ppm CO, the rise

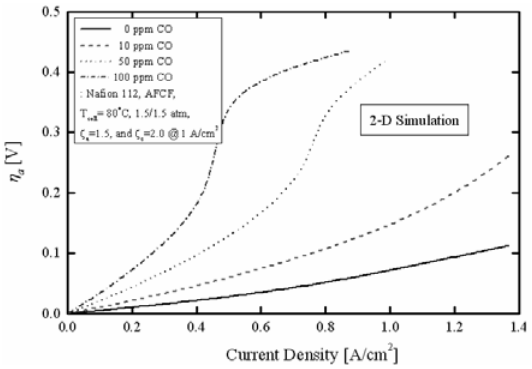

Fig. 3. Anode overpotential as a function of the current density with various concentration of CO in the anode feed gas (calculated by the 2-D simulations under fully humidified air and H_2, Nafion112).

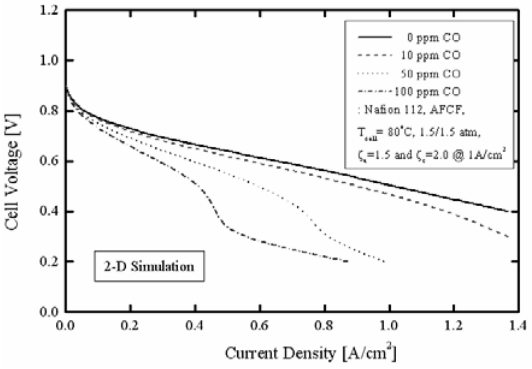

Fig. 4. Polarization curves with various concentration of CO in the anode feed gas (calculated by the 2-D simulations under fully humidified air and H_2, Nafion112).

of anode overpotential becomes significant, indicating that the cell performance is severely affected by CO poisoning. When the current density is further increased (more than 0.5A/cm^2 for the 100ppm CO case), the anodic polarization is flattened due to much increased rate of CO electro-oxidation. The polarization curves obtained by the 2-D simulations are shown in Fig. 4, compared to the cases with various CO concentrations ranging from 0ppm to 100ppm CO. The same classification of three regimes is observed, in accordance with Fig. 3.

Fig. 5 displays the contour plots of the CO concentration field from the anode gas channel to catalyst layer at V_{cell} = 0.4V, 0.3V and 0.2V with 100ppm CO in the anode feed streams. The consumption of CO by electrochemical oxidation was visible at 0.4 V; CO is oxidized by roughly 55% at V_{cell} = 0.3V (I = 0.505A/cm^2) and about 90% at V_{cell} = 0.2V (I = 0.871/cm^2). So these results are consistent with those of Figs. 3 and 4. It is shown from Fig. 3 that the increase in anodic polarization due to CO poisoning is significantly alleviated at I = 0.5A/cm^2. This can now be attributed to the fact that considerable CO is already oxidized at this current density of 0.5A/cm^2. Fig. 6 shows variations of the fractional coverage for H_2 and CO as functions of the cell voltage for the 10 ppm CO, 50ppm CO, and 100ppm CO cases. The higher CO coverage and accordingly lower hydrogen coverage are predicted as CO concentration of anode feed streams becomes higher. In addition, for the 100 ppm CO case, it is clearly seen that the fractional coverage of CO starts to decrease roughly at V_{cell} = 0.4 V where 55% of 100ppm CO was oxidized (see Fig. 5).

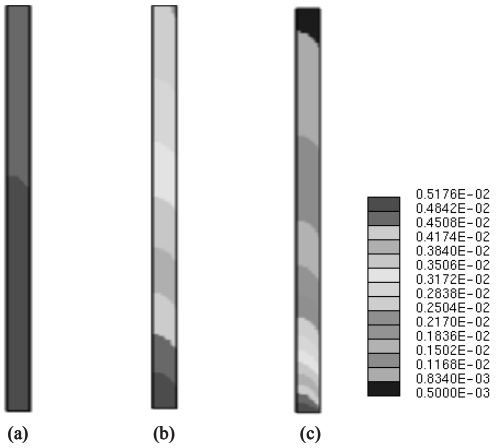

Fig. 5. Contour plots of CO concentration (Anode gas channel through Anode catalyst layer): (a) V_{cell}=0.4 V; I=0.463 A/cm^2, (b) V_{cell}=0.3 V; I=0.505 A/cm^2 ,and (c) V_{cell}=0.2 V; I=0.871 A/cm^2 (100 ppm CO, obtained from 2-D simulations).

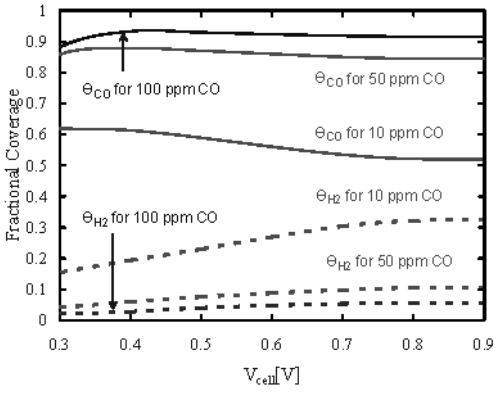

Fig. 6. Fractional coverage of H_2 and CO as functions of the cell voltage with various concentration of CO in the anode feed gas (calculated by the 2-D simulations under fully humidified air and H_2, Nafion112).

4.2 Multi-dimensional effects

The numerical simulations performed by Springer et al. (2001) were based on a pseudo 2-D model, in which a 1-D model is used to describe the reaction-diffusion problem within gas diffuser at each section of the flow channel, and another set of ODEs is employed to keep track of varying species concentrations (averaged) inside the gas channel. There is clearly a multi-dimensional effect from the CO concentration contour shown in Fig. 5. Moreover, there is a large concentration gradient in the transverse direction, rendering the pseudo 2-D approach of Springer

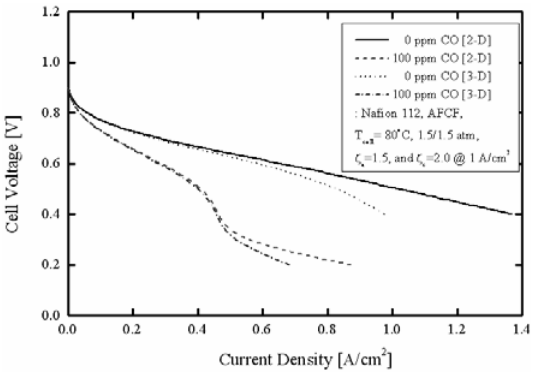

Fig. 7. The multi-dimensional effects of polarization curves for 0ppm CO and 100ppm CO (Nafion112, fully humidified H_2 and air).

et al. (2001) invalid. Finally, the rib effect on the reactant diffusion can only be captured by fully three-dimensional simulations. It is thus of interest to compare the 2-D simulation results with a fully 3-D calculations as shown in Fig. 7. As expected, the current density calculated from the 3-D simulations is lower than that from 2-D simulation due to the rib effects.

5. Conclusions

The goal of the present CO poisoning analysis was to find ways to minimize the CO poisoning effects in a PEMFC. For this purpose, detailed CO poisoning mechanisms consisting of four chemical/electrochemical processes in the anode side were successfully implemented in a 3-D, electrochemical and transport fully coupled PEMFC model. It is clearly demonstrated that these simulation results strongly resemble experimental observations in the literature. In particular, the model correctly captured the three distinctive regions characterizing CO poisoning in the plot of voltage-current relation, i.e., the polarization curve. According to the numerical simulation results, these three distinctive regions appear in the cases of 50 and 100ppm CO, indicating that the CO feed gas levels are extremely detrimental to cell performance. On the other hand, 10ppm CO level has shown negligible reduction in PEMFC performance and is thus acceptable for the PEMFC based on pure platinum catalyst, which agrees with the conclusions drawn by Brown (2001). The predictive capability for CO poisoning by using a comprehensive PEMFC model is a useful tool to find methods to mitigate the effect of CO poisoning on PEMFCs.

Acknowledgments

Thanks are due to Prof. Chao-Yang Wang at the Pennsylvania State University for useful discussions on the CO poisoning analysis.

Nomenclature

a : Water activity or effective catalyst area per unit of total volume, m^2/m^3
A : Area, m^2
b_c : Tafel slope for CO electro-oxidation, V
b_h : Tafel slope for H_2 electro-oxidation, V
b_{fc} : Back-to-forward CO adsorption ratio, atm
b_{fh} : Back-to-forward H_2 adsorption ratio, atm
C : Molar concentration, mol/m^3
D_k : Mass diffusivity of species k, m^2/s
F : Faraday constant, 96487 C/mol
i_0 : Exchange current density, A/m^2
j : Transfer current density, A/m^3
k_{ec} : Exchange current density of CO electro-oxidation, A/m^2
k_{eh} : Exchange current density of H_2 electro-oxidation, A/m^2
k_{fc} : Forward CO adsorption rate times 2F, $A/m^2 \cdot atm$
k_{fh} : Forward H_2 adsorption rate times 2F, $A/m^2 \cdot atm$
K : Hydraulic permeability, m^2
M : Molecular weight, kg/mol
n : Number of electrons in electrochemical reaction or order of H2 adsorption
P : Pressure, Pa
R : Universal gas constant, 8.314J/(mol K)
s : Stoichiometry coefficient in electrochemical reaction
S : Source term in transport equation
T : Temperature, K
$\boldsymbol{u}$: Fluid velocity and superficial velocity in porous medium, m/s
V_{cell} : Cell potential, V
x_k : Mole fraction of species k

Greeks

α : Transfer coefficient
ε : Volume fraction of gaseous phase in porous region
ϕ : Phase potential, V
η : Overpotential, V
θ : Fractional coverage
μ : Viscosity, kg/ (m s)
ρ : Density, kg//m^3
τ : Viscous shear stress, N/m^2
κ : Ionic conductivity, S/m
ξ : Stoichiometry flow ratio

Superscripts

eff : Effective value in porous region

Subscripts

a : Anode
c : Cathode
CO : Carbon monoxide
H2 : Hydrogen

e : Electrolyte
k : Species index
Φ : Potential equation
u : Momentum equations

References

[1] H. Oetjen, V. M. Schmidt, U. Stimming and F. Trila, Performance data of a proton exchange membrane fuel cell using H_2/CO as fuel gas, *J. Electrochem. Soc.,* 143 (1996) 3838-3842.

[2] T. E. Springer, T. Rockward, T. A. Zawodzinski and S. Gottesfeld, Model for polymer electrolyte fuel cell operation on reformate feed: effects of CO, H_2 dilution, and high fuel utilization, *J. Electrochem. Soc.,* 148 (2001) A11-A23.

[3] M. Murthy, M. Esayian, A. Hobson, S. MacKenzie, W. K. Lee and J. W. Van Zee, Performance of a polymer electrolyte membrane fuel cell exposed to transient CO concentrations, *J. Electrochem. Soc.,* 148 (2001) A1141-A1147.

[4] L. Brown, A comparative study of fuels for on-board hydrogen production for fuel-cell-powered automobiles, *Int. J. Hydrogen Energy,* 26 (2001) 381-397.

[5] J. Divisek, H. F. Oetjen, V. Peinecke, V. M. Schmidt and U. Stimming, Components for PEM fuel cell systems using hydrogen and CO containing fuels, *Electrochimica Acta,* 43 (1998) 3811-3815.

[6] J. Zhang, T. Thampan and R. Datta, Influence of anode flow rate and cathode oxygen pressure on CO poisoning of proton exchange membrane fuel cells, *J. Electrochem. Soc.,* 149 (6) (2002) A765-A772.

[7] G. A. Camara, E. A. Ticianelli, S. Mukerjee, S. J. Lee and J. McBreen, The CO poisoning mechanism of the hydrogen oxidation reaction in proton exchange membrane fuel cells, *J. Electrochem. Soc.,* 6 (2002) A748-A753.

[8] S. Um, C. Y. Wang and K. S. Chen, Computational fluid dynamics modeling of proton exchange membrane fuel cells, *J. Electrochem. Soc.,* 147 (2000) 4485-4493.

[9] H. Ju and C. Y. Wang, Experimental validation of a PEM fuel cell model by current distribution data, *J. Electrochem. Soc.,* 151 (2004) A1954-A1960.

[10] H. Ju, H. Meng and C. Y. Wang, A single-phase, non-isothermal model for PEM fuel cells, *Int. J. Heat Mass Transfer,* 48 (2005) 1303-1315.

[11] T. E. Springer, T. A. Zawodzinski and S. Gottesfeld, Modeling of polymer electrolyte fuel cell performance with reformate feed stream: effects of low levels of CO in hydrogen, *The Electrochemical Society Proceedings Series,* PV 97-13 (1997) 15-24.